Journal of Applied Electrochemistry (2006) 36:385–394
DOI 10.1007/s10800-005-9082-y

Hardening effect induced by incorporation of SiC particles in nickel electrodeposits

E.A. PAVLATOU, M. STROUMBOULI, P. GYFTOU and N. SPYRELLIS*
Laboratory of General Chemistry, School of Chemical Engineering, National Technical University of Athens, 9, Heroon Polytechniou Str., Zografos Campus, Athens, GR-15780, Greece
*(*author for correspondence, tel.: +30-210-7723085, fax: +30-210-7723088, e-mail: nspyr@chemeng.ntua.gr)*

Received 10 May 2005; accepted in revised form 30 September 2005

Key words: composites, microhardness, nickel electrodeposits, pulse plating, silicon carbide, texture

Abstract

Pure Ni and nickel matrix composite electrocoatings containing micron- and nano-SiC particles (1 μm and 20 nm respectively) were produced under direct and pulse current conditions from an additive-free Watts type bath. The effect of the particle size, codeposition percentage of SiC and type of imposed current on the microhardness as well as on the microstructure of the electrodeposits were investigated. Ni/SiC composite deposits prepared under either direct or pulse current conditions exhibited a considerable strengthening effect with respect to pure Ni coatings. The improved hardness of composite coatings was associated to specific structural modifications of Ni crystallites provoked by the adsorption of H^+ on the surface of SiC particles, thus leading to a (211) texture mode of Ni crystal growth. Pulse electrodeposition significantly improved the hardness of the Ni/SiC composite coatings, especially at low duty cycles, in which grain refinement and higher SiC incorporation (vol. %) was achieved. The enhanced hardness of Ni/nano-SiC deposits, as compared to Ni/micron-SiC composites, was attributed to the increasing values of the number density of embedded SiC particles in the nickel matrix with decreasing particle size. In addition, the observed hardening effects of the SiC particles might be associated to the different embedding mechanisms of the particles, which could be characterized as inter-crystalline for micron-SiC and partially intra-crystalline for nano-SiC particles.

1. Introduction

The electrolytic codeposition of solid particles, such as hard oxides, carbides, nitrides, or even polymeric particles, with metals or alloys has been the subject of investigation and industrial applications for some decades [1–3]. Recently, a new generation of metal matrix composites reinforced by micron and nano-sized particles has attracted scientific and technological interest due to the recent availability of ever decreasing particle sizes and due to the resulting enhanced properties of the coatings, such as hardness, wear and corrosion resistance [4–9].

Silicon carbide nickel matrix coatings have been extensively studied and have gained widespread use for protection of friction inside parts of cylinders in the automotive industry. Considerable research has been mainly focused on the impact of the electrodepostion parameters: electrolysis conditions (composition of the electrolytic bath, presence of additives, pH value), current conditions (type of imposed current and values of the current density) and properties of the reinforcing particles (size, surface properties, concentration and type of dispersion in the bath) on the electrolytic codeposition process of SiC with Ni, as well as the properties of the composite electrocoatings [4–22]. In general, it has been observed that the amount of embedded SiC particles increases with both increasing concentration of suspended SiC particles and surfactant or organic additives in the electrolyte [14–18]. It has also been reported that a decrease in the SiC particle size affects the wear and corrosion resistance in a positive way [6, 9, 17]. However, the reduction of particle size decreases the codeposition content of the particles [6, 11, 15]. Thus, it seems that the particle size plays an important role in the electrocodeposition process and hence in the mechanical properties of the Ni/SiC composite coatings. Moreover, recent research has pointed out that the physico-chemical properties of the SiC particles are crucial to the understanding of the codeposition mechanism [10–11, 19–21].

Relatively less research work has been done to examine the effect of the current type on the codeposition process of the composite Ni/SiC electrocoatings [4, 7, 12, 13, 22], although a significant number of reports have shown that the microstructure and properties of pure Ni deposits may be effectively altered under specific pulse current conditions [23–26]. Pulse electrodeposition has been found to be an effective means of perturbing the adsorption–desorption

phenomena occurring at the electrode–electrolyte interface and hence the electrocrystallization process. In addition, pulse plating permits higher current densities than the limiting direct current density to be attained and thus nanocrystalline Ni deposits could be produced [13, 24]. In the case of Ni/SiC codeposits, the application of pulse current techniques results in the production of composite coatings with higher percentages of incorporation, and a more uniform distribution of SiC particles in the Ni matrix than those attained under direct current regime [4, 5, 12, 13].

It is noteworthy that, as mentioned above, although there is a plenty of research work concerning either the effect of operating conditions on the amount of codeposited SiC particles or and the resulting mechanical properties of composite coatings, the effect of the embedded particles on the microstructure of the coatings and, consequently, the relation between structure and properties has been investigated to a limited extent [9, 12, 20]. In the present study, the electrolytic codeposition of micron- or nano-sized SiC particles with Ni from an additive free nickel Watts solution by applying either direct or pulse electroplating, was investigated. The microstructure, the preferred orientation of nickel crystallites and the microhardness of the coatings were determined. Pure Ni deposits were also produced under the same experimental conditions for comparison. The effect of the particle size, codeposition percentage of SiC and type of imposed current on the microhardness, as well as on the microstructure of the electrodeposits were examined. A hardening mechanism is also proposed in order to provide further insight into the codeposition of SiC with Ni.

2. Experimental details

Pure Ni and composite Ni/SiC coatings were electrolytically deposited from an additive-free nickel Watts solution. The electrodeposition experiments were performed on rotating disk electrodes (RDEs) with a rotation velocity of 200 rpm under either direct or pulse current conditions. In the case of Ni/SiC composite deposits, the selected commercial SiC powders with a mean diameter of 1 μm (β-SiC, Alfa Aesar) or 20 nm (β-SiC, Marketech International INC), respectively, were added to the bath and maintained in suspension by continuous magnetic stirring with a rate of 250 rpm for at least 12 h before codeposition. The substrates were brass discs that were mechanically polished and chemically cleaned in an ultrasonic agitated bath before deposition. The anode, which was a nickel foil of 99.9% purity, was positioned on the side of the electrolytic cell.

During electrodeposition the temperature of the plating solution was maintained at 50 ± 1 °C, the initial pH of the electrolyte was adjusted to a constant value of 4.4 and the solution was agitated by the use of a 250 rpm magnetic stirrer placed at the cell bottom. In pulse deposition experiments the frequency (ν) of the imposed pulses was set at the value of 0.1 Hz, while the duty cycle (d.c.) of the pulses [*i.e.* d.c. $= T_{on}/(T_{on} + T_{off})$, where T_{on} is the time period the pulses are imposed, and T_{off} is the relaxation time] varied between 10 up to 90%. The composition of the plating solution with a total volume of one liter and the deposition parameters are given in Table 1.

After electrolysis, the deposits were ultrasonically cleaned in distilled water for 10 min in order to remove loosely adsorbed SiC particles from the surface. The thickness of the produced coatings was above 50 μm.

Measurements of the Vickers microhardness (HV in kgf mm^{-2}) of pure nickel and Ni/SiC composite deposits were performed on the surface by using a Reichert microhardness tester under 50 g load and the corresponding final values were determined as the average of 10 measurements. The thickness of the coatings and the selected load were chosen so as to avoid any substrate effect on the microhardness value measured [27].

The preferred crystalline orientation of the Ni was examined by applying X-ray diffraction (XRD) technique utilizing a Siemens D-5000 diffractometer operating with a Cu-K_α radiation. Morphological and microstructural characterizations of the deposits involved scanning electron microscopy (SEM, JSM-6300) and transmission electron microscopy (TEM-Philips CM12). Moreover, the amount of embedded SiC particles was evaluated by using energy dispersive X-ray spectroscopy (EDS, Oxford Instruments) and the determined amount of codeposited particles SiC with Ni resulted from the mean value of at least three measurements for each deposit.

3. Results and discussion

3.1. *Pure Ni deposits*

Figure 1 shows a significant influence of the imposed current type on the microhardness of pure Ni deposits. The hardness of Ni deposits prepared under pulse

Table 1. Overview of the electrodeposition parameters for preparation of pure Ni and composite Ni/SiC coatings

Solution composition	
Electrolyte (Watts)	
$NiSO_4 \cdot 6H_2O$	300 g l^{-1}
$NiCl_2 \cdot 6H_2O$	35 g l^{-1}
H_3BO_3	40 g l^{-1}
SiC powder	20 g l^{-1}
(mean diameter of 1 μm and 20 nm)	
Electrodeposition conditions	
pH	4.40
Temperature	50 °C
Substrate	Brass disc (diameter 25 mm)
Cathode rotation rate (ω)	200 rpm
Anode	Ni foil
Agitation of electrolyte	Magnetic stirring
Current density	5 A dm^{-2}
Type of current	Direct (DC) or Pulse (PC)
Duty cycle (d.c.)	10, 30, 50, 70 and 90%
Pulse frequency (ν)	0.1 Hz

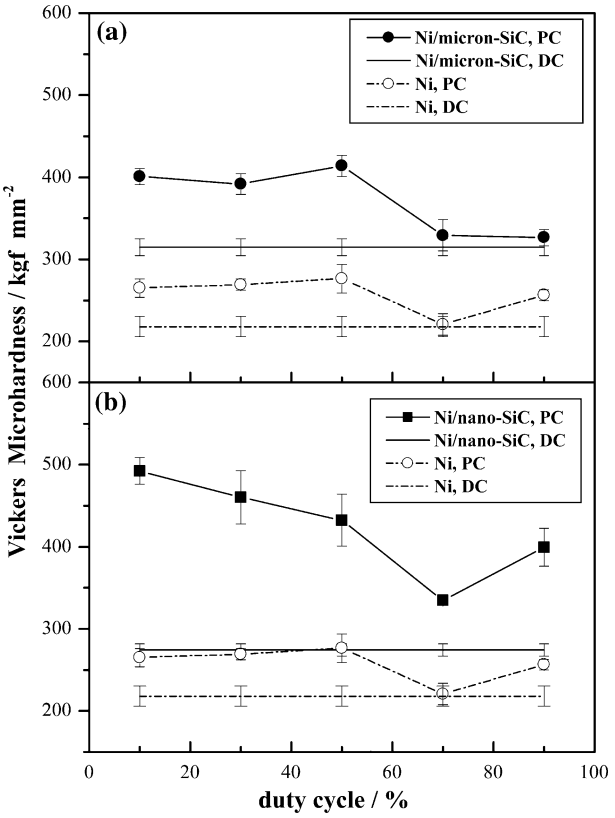

Fig. 1. Vickers microhardness values of pure Ni, (a) Ni/micron-SiC and (b) Ni/nano-SiC deposits, prepared under DC and PC conditions with a constant value of pulse frequency $\nu = 0.1$ Hz, *vs.* duty cycle (d.c.).

current (PC) conditions varies with duty cycle and reaches a maximum value of ~270 kgf mm^{-2} and is always higher than the corresponding result for deposits prepared under direct current (DC) conditions which is ~210 kgf mm^{-2}. Under a pulse regime, the hardness of the deposits is in general enhanced by decreasing the duty cycle value at constant frequency of pulses, which means that deposits with the highest HV values are those prepared under low duty cycles.

The XRD diagrams of all pure Ni deposits prepared under both direct and pulse current conditions revealed a (100) preferred crystalline orientation as presented in Figure 2. According to the perturbations of nickel electrocrystallization due to the pulse electrolysis, our experimental pulse plating conditions correspond to the region of inhibition of nickel crystal growth by adsorption of anions (or other foreign species) from the bulk solution on the metallic surface [23]. This reinforced adsorption process of anions provokes a poisoning of the growth sites and implies that a re-nucleation process takes place during the next pulse. In such a case the pulse plated deposits have smaller crystallites, containing much more structural defects and consequently higher HV values are expected than for those prepared under DC conditions. It has been demonstrated that this inhibition is more intense at low duty cycles [23] and this may explain the finding that the highest HV values are achieved at increasing values of relaxation time. These observations are also in agreement with recent studies, in which Ni deposits with finer grain size and enhanced hardness may be obtained by applying pulse plating at low duty cycles compared with those prepared under direct current electrodeposition [25, 26, 28].

3.2. *Ni/SiC composite coatings*

3.2.1. *Hardness improvement due to the reinforcement*

Ni/SiC composite deposits prepared under either direct or pulse current conditions have higher Vickers microhardness values than pure nickel deposits produced under similar conditions, as depicted in Figures 1(a) and (b). This increasing of the HV values may be attributed to two different effects (apart from the strengthening effects by the reinforcing phase itself): firstly to the reduction of the grain size, and secondly to the structural modification of Ni crystallites expressed through the alteration of the preferred orientation. Figure 3 shows the surface morphology of pure Ni and composite Ni/SiC deposits both prepared under pulse plating conditions. The typical shape of (100) nickel crystallites, which may exceed a size of 10 μm, is depicted in Figure 3(a). In contrast, Figure 3(b) demonstrates the characteristic shape of (211) Ni crystallites with grain size less than 2 μm [29]. The textural modification revealed in the SEM micrographs is also distinct in the corresponding XRD diagrams of the coatings [Figures 2(b) and 4(b)]. It is apparent that the diffraction pattern of the pure Ni deposit is characterized by an intense (200) diffraction line corresponding to a (100) texture (Figure 2(b)), while those of Ni/SiC deposits exhibit a reinforcement of (311) and (111) lines accompanied with an attenuation of the (200) line (Figure 4). It is of interest to note that the reinforcement of the lines (311) and (111) is attributed to a dispersed (211) orientation [30]. Moreover, the microstructure corresponding to the (100) texture is associated to deposits that present maximum ductility [31] and the minimum hardness and internal stresses [32, 33]. Hence, it is obvious that the embedding of SiC particles in the Ni matrix modifies the soft-mode (100) texture to a mixed preferred orientation of Ni crystallites through (100) and (211) axis. This textural modification is more pronounced in the case of micron-SiC composite coatings (Figure 4b).

The reduction of the grain size of Ni crystallites due to the presence of SiC particles is also discernible in SEM micrographs of composite deposits (Figure 5) compared with those of pure Ni deposits (Figure 3a). This experimental finding was also reported for the case of Ni/nano-SiC composites, which exhibited improved wear and corrosion resistance compared with pure Ni coatings [15]. Moreover, Zimmerman et al. [7] reported that nickel, deposited by pulsed electrolysis from a Watts bath containing saccharin, demonstrated grain sizes ranged from 9.9 to 40 nm. In Ni/micron SiC deposits the grain size was reduced to the 10.3–15.0 nm range and a significant increase in the hardness values was evident in comparison with pure Ni deposits [7].

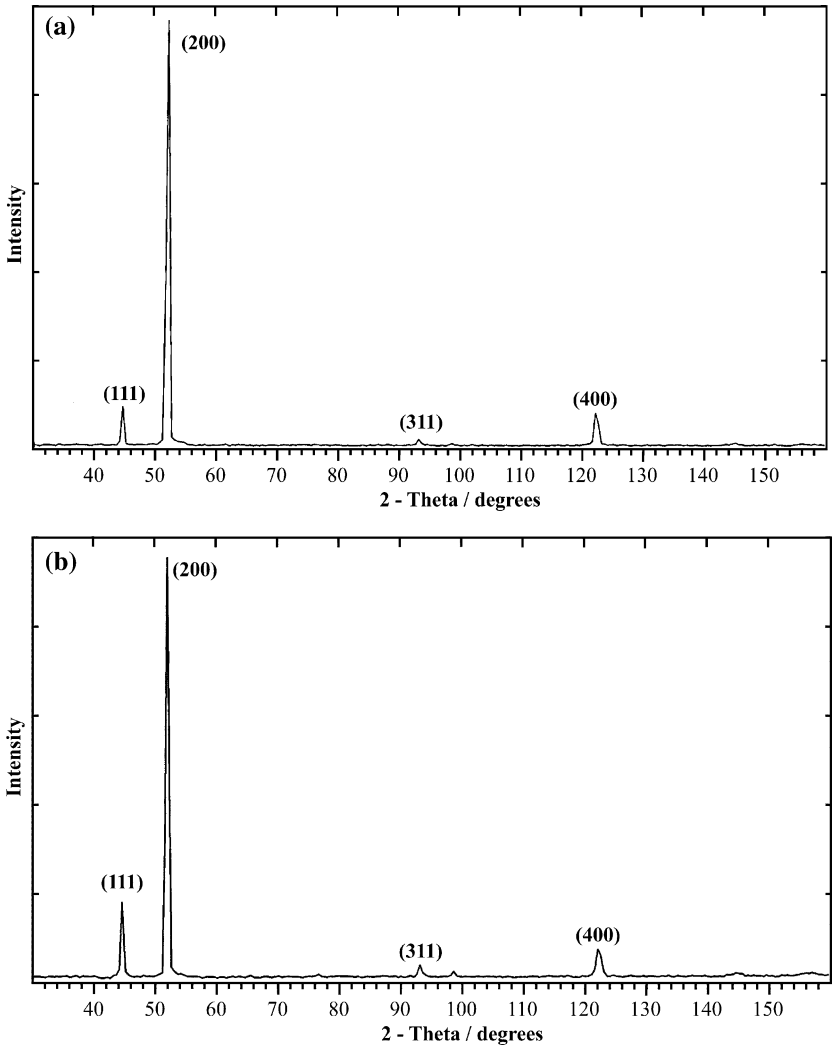

Fig. 2. XRD patterns of pure Ni coatings prepared under (a) DC and (b) PC conditions at d.c. = 30% and ν = 0.1 Hz.

Electrochemical impedance spectroscopy measurements [20] revealed that the embedding of partly hydrophobic SiC particles blocked a part of the metallic surface causing a current decrease, and thus new growth centers were produced, resulting in smaller Ni crystal size.

All these studies, as well as the previous mentioned experimental data, indicate that SiC codeposition significantly influences the crystal growth mode of Ni and in turn modifies the deposit mechanical properties. Several researchers [8, 20] propose that codeposition of SiC particles perturbs the crystal growth of the Ni matrix by inducing an increase in the number of the nucleation sites and, consequently, a reduction in the crystallite size occurs. This effect cannot be explained only by the simple presence of SiC particles, if they are considered as physico-chemically inert particles. In fact, the particles intervene by changing the catholyte composition by adsorption of H^+ [34], resulting in local alkalization of the cathode/electrolyte interface and, therefore, leading to a (211) mode of crystal growth [35]. Moreover, this modified composition of the catholyte inhibits Ni growth and provokes re-nucleation and hence results in a microcrystalline metal matrix. Also, this inhibition in synergy with the incorporation effect of SiC particles simultaneously provokes an increasing number of crystalline dislocations, as depicted in Figure 6. The overall microstructure change results in the production of Ni/SiC composite deposits with significantly increased hardness in comparison with pure Ni deposits prepared under similar experimental conditions. The improved hardness of the composite coatings is actually linked to a change in grain size and structure of Ni crystallites.

3.2.2. *Effect of pulse plating*

For both Ni/micron-SiC and Ni/nano-SiC composite coatings, the use of pulse current results in deposits with considerable higher HV values in comparison with deposits prepared under direct current conditions (Figure 1). It is noteworthy that Ni/nano-SiC deposits prepared under PC conditions demonstrate HV values about two times higher than those obtained under DC conditions, attaining a maximum value of $\sim$500 kgf mm^{-2}. According to our previous studies, an improvement in hardness in composite Ni/SiC deposits is expected since the application of pulse

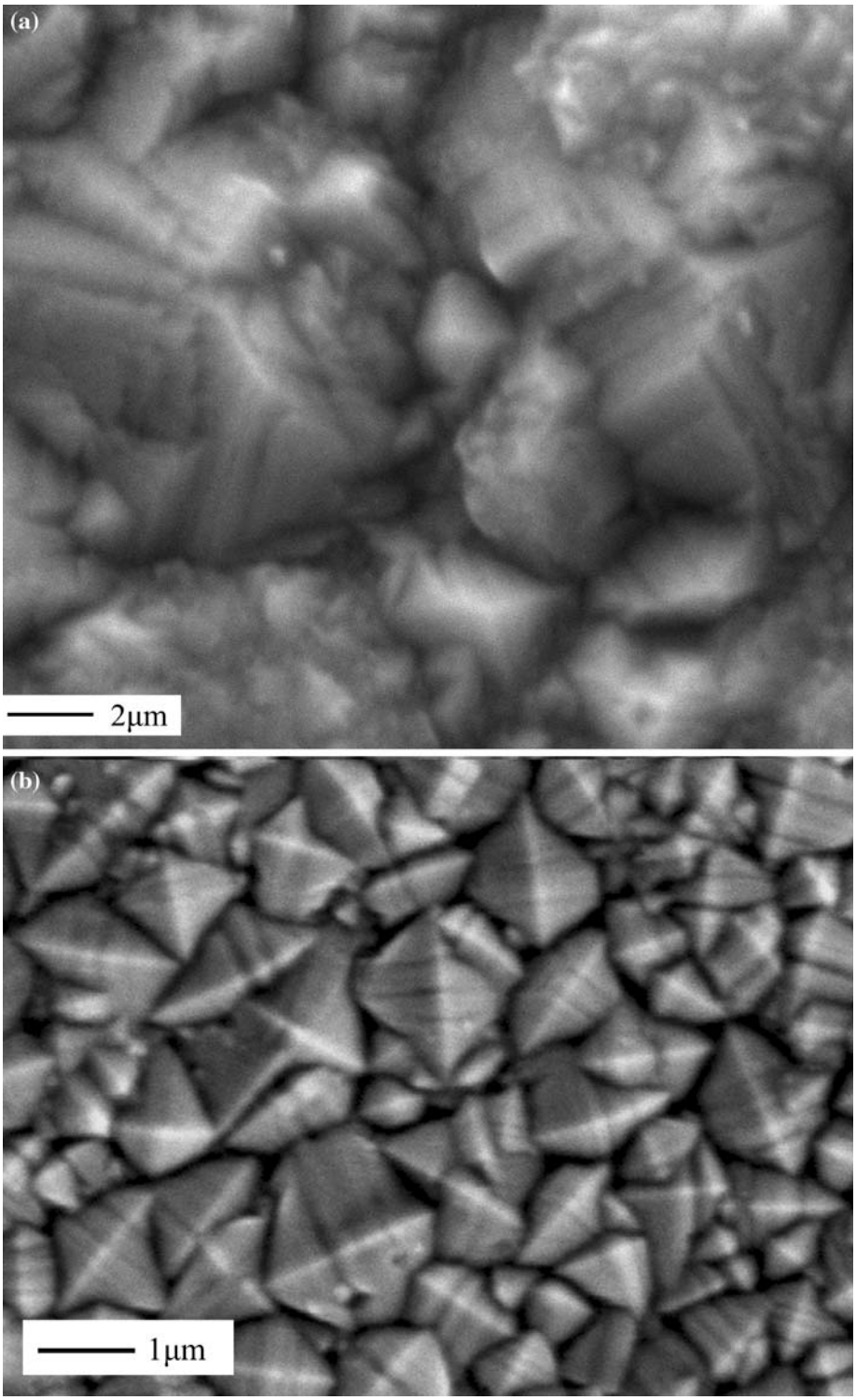

Fig. 3. SEM micrographs presenting the typical morphology of Ni crystallites oriented through (a) the (100) axis from a pure Ni deposit prepared under PC regime (d.c. = 90%) and (b) the (211) axis from a selective area of a composite Ni/micron-SiC deposit prepared under PC conditions (d.c. = 50%).

current results in coatings with uniform SiC particle distribution in the Ni matrix, as well as higher percentages of embedded SiC particles relative to those obtained under direct current regimes [12, 36, 37]. Moreover, it has been reported that the use of rectangular waveform current with long relaxation time induces a high nucleation rate and thus favors fine grains of Ni in Ni/SiC deposits [22]. Additionally, for these composite Ni/SiC coatings, the variation of the HV values as a function of the duty cycle follows the same trend observed for pure Ni deposits: the highest HV values are achieved by applying pulses at low duty cycles. The observed hardening effect of pulse parameters may be attributed to the significant grain refinement obtained at pulse-off times longer than pulse on-times [24, 26].

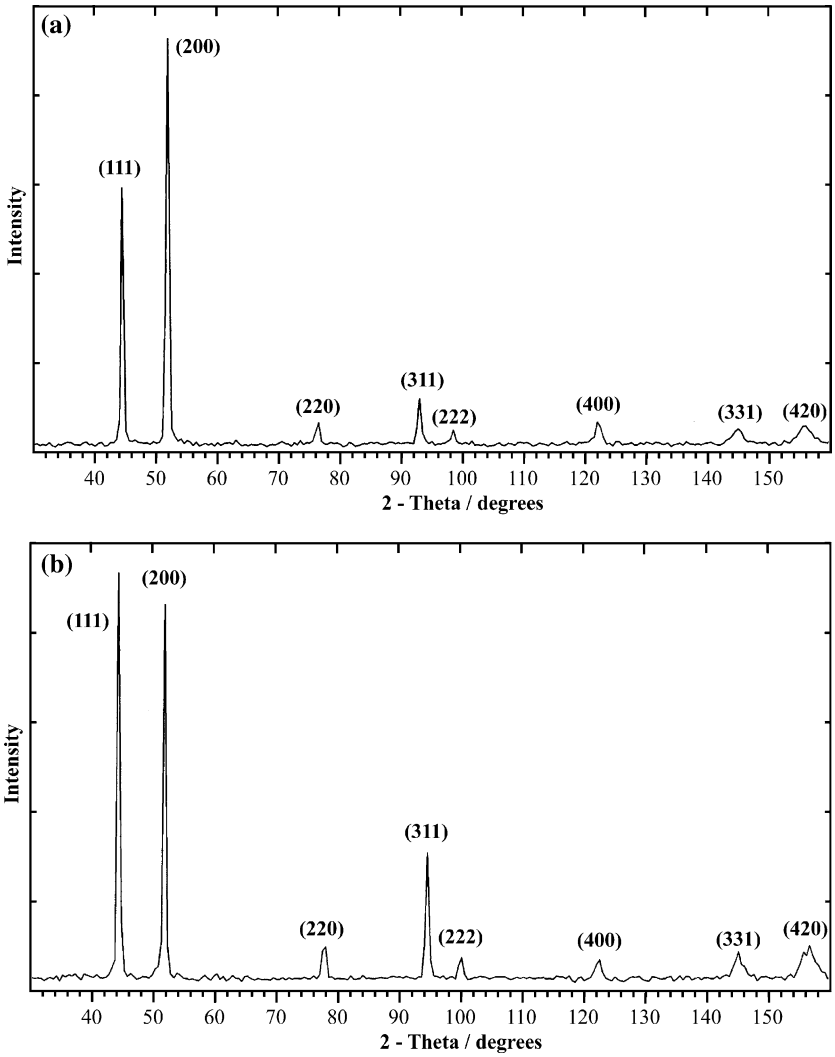

Fig. 4. XRD patterns of (a) Ni/nano-SiC and (b) Ni/micron-SiC composite coatings both prepared under PC conditions at d.c. = 30% and $\nu = 0.1$ Hz.

3.2.3. *Effect of particle size*

Regarding the effect of the particle size on hardness values, it is apparent that the higher HV values are those of Ni/nano-SiC composites (Figure 1). It is known that the hardness of metal matrix composites depend on the amount and the size of the dispersed phase, apart from the mechanical characteristics of the matrix, particles and interfaces. In general, several studies have shown that the microhardness of Ni/SiC coatings increases with increasing amount of SiC particles in the deposits [6, 7]. According to our results it seems that this is valid only in the case where the particle size is the same. Moreover, the HV values depend strongly on the size of the embedded particles and nano-sized particles reached higher HV values with lower codeposition percentage vol. % of SiC, relative to those of Ni/micron-SiC deposits (Figure 7). This result emphasizes the importance of considering not only the vol. % of embedded particles, when comparing the effect of particle size on codeposition, but also the data in terms of number density of embedded particles [6]. In such a case, the difference of four orders of magnitudes in the number of particles between the deposits of Ni/micron and Ni/nano SiC may account for the increasing HV values of the latest composite coatings. It is noteworthy that the general tendency of our data at constant SiC particle size is that with increasing number of particles in the coatings the hardness value is increased, and the highest values are observed at deposits prepared at low duty cycles (e.g. 10%) wherein the highest vol. % or number density of embedded particles, *i.e.* 16.2 and 4.7 vol. % for micron and nano-composite deposits, respectively, is achieved.

In order to analyze further mechanical properties, such as hardness, the inter-particle spacing λ is calculated; this depends not only on the vol. % but also on the size and distribution of the particles, and predetermines the obstruction to dislocation movement and resistance to deformation. Both composite coatings are characterized by values less than 3 μm for micron particles and 0.2 μm for nano-particles, assuming that the SiC particles are monodisperse, spherical and uniformly distributed in the matrix. Thus, the hardness increase noted in these composite coatings may be

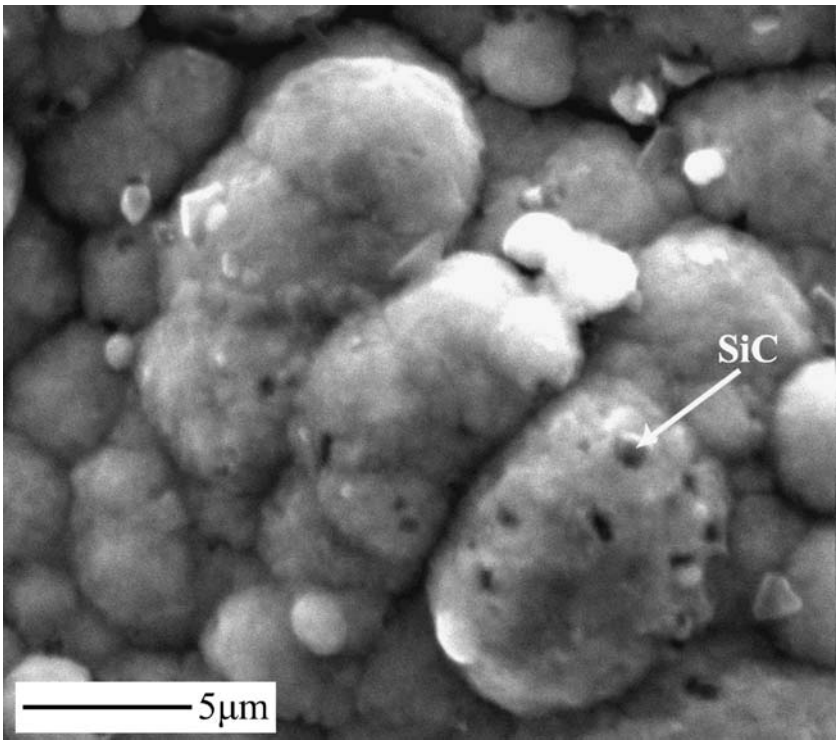

Fig. 5. SEM micrograph illustrating the microcrystalline aggregates of Ni and the inter-crystalline embedding of SiC particles in the Ni matrix of a Ni/micron-SiC coating produced under PC conditions (d.c. = 10%).

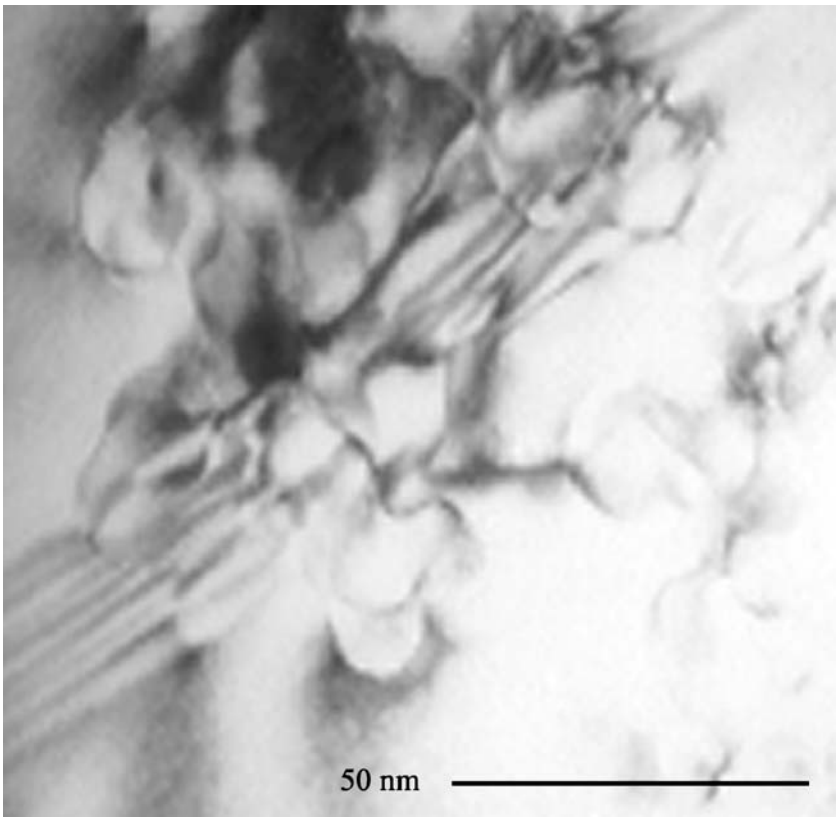

Fig. 6. TEM image of a cross section of a Ni/nano-SiC deposit prepared at d.c. = 90% presenting the Ni crystalline dislocations induced by the embedding of SiC particles in the metallic matrix.

linked to a dispersion-strengthening mechanism, in which the matrix carries the load and the fine particles impede the motion of dislocations. It should be noticed that, in order to obtain a dispersion-strengthening effect, it is crucial to achieve a uniform embedding of non-agglomerated sub-micron particles in the matrix.

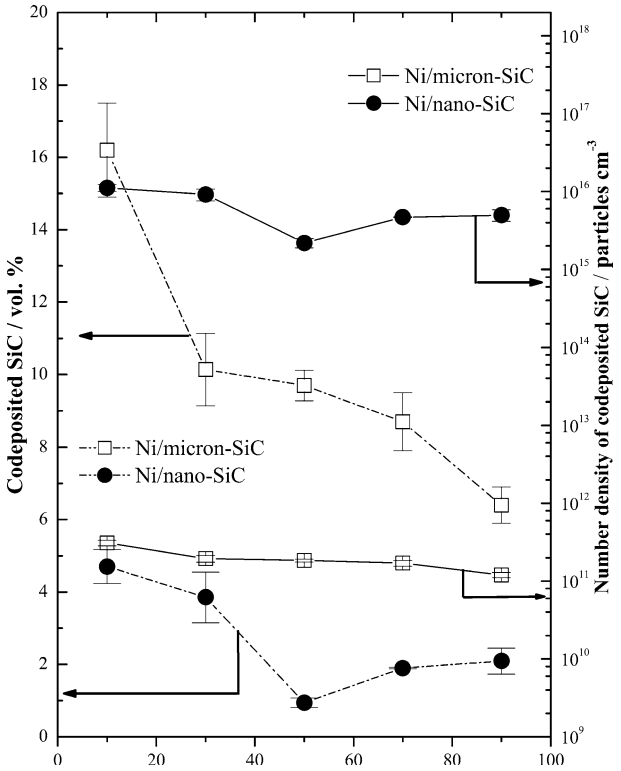

Fig. 7. Volume percentage and number density of SiC particles codeposited with Ni at different sizes *vs.* duty cycle (d.c.).

The SEM micrographs (Figure 8) indicate a uniform dispersion of the particles in the matrix in the case of micron (Figure 8(a)), as well nano-particles (Figure 8(b) and (c)).

Moreover, the observed increasing HV values of Ni/nano-SiC as compared to Ni/micron-SiC deposits may also be attributed to the different types of incorporation mechanism. In the case of micron-SiC particles the embedding mechanism is *inter-crystalline*, which means that micron-SiC particles are incorporated at the borders and edges of the Ni crystallites, as shown in Figure 5. In contrast, in the case of nano-SiC particles, the embedding mechanism is partially *intra-crystalline*, as verified by TEM observations (Figure 9). Figure 9 demonstrates that in composite Ni/SiC deposits some nano-SiC particles are embedded at the borders of Ni crystallites (*e.g.* particle (b)-SiC), as well as inside the Ni crystals (*e.g.* particle (a)-SiC).

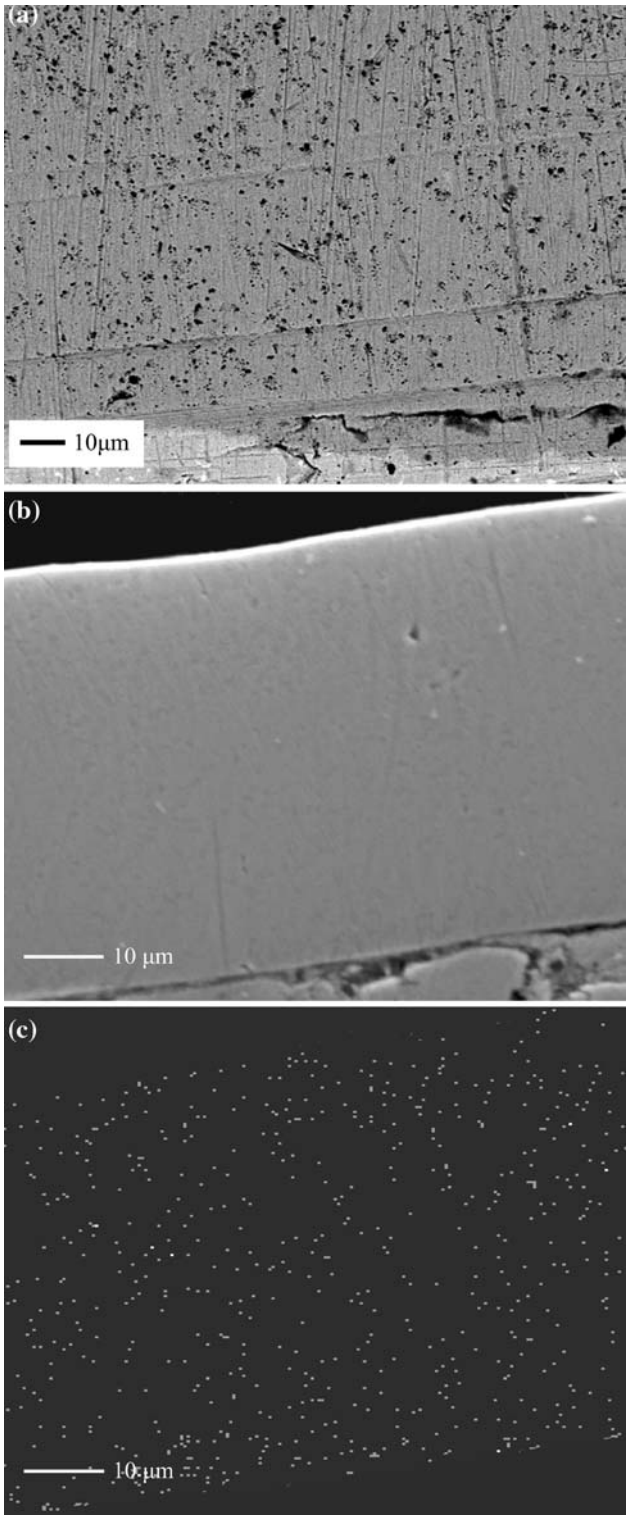

Fig. 8. (a) Backscattered SEM micrograph of the cross-profile of Ni/micron-SiC deposit prepared in the PC regime (d.c. = 30%), (b) and (c) SEM image of the cross-profile and Si mapping image of Ni/nano-SiC deposit prepared under PC conditions (d.c. = 90%). All these micrographs show the uniform distribution of both kinds of SiC particles in the Ni matrix.

4. Conclusions

The hardness of pure Ni and composite Ni/SiC deposits was shown to depend on the type of imposed current, the size of the embedded particles, the codeposition percentage of particles and the microstructural modifications induced by the codeposition of SiC particles, as well as by the application of specific pulse current conditions. Pure Ni deposits with enhanced hardness and finer grain size were produced by applying pulse plating at low duty cycles compared to those prepared under direct current electrodeposition.

The codeposition of SiC particles leads to a considerable strengthening of Ni/SiC composite deposits

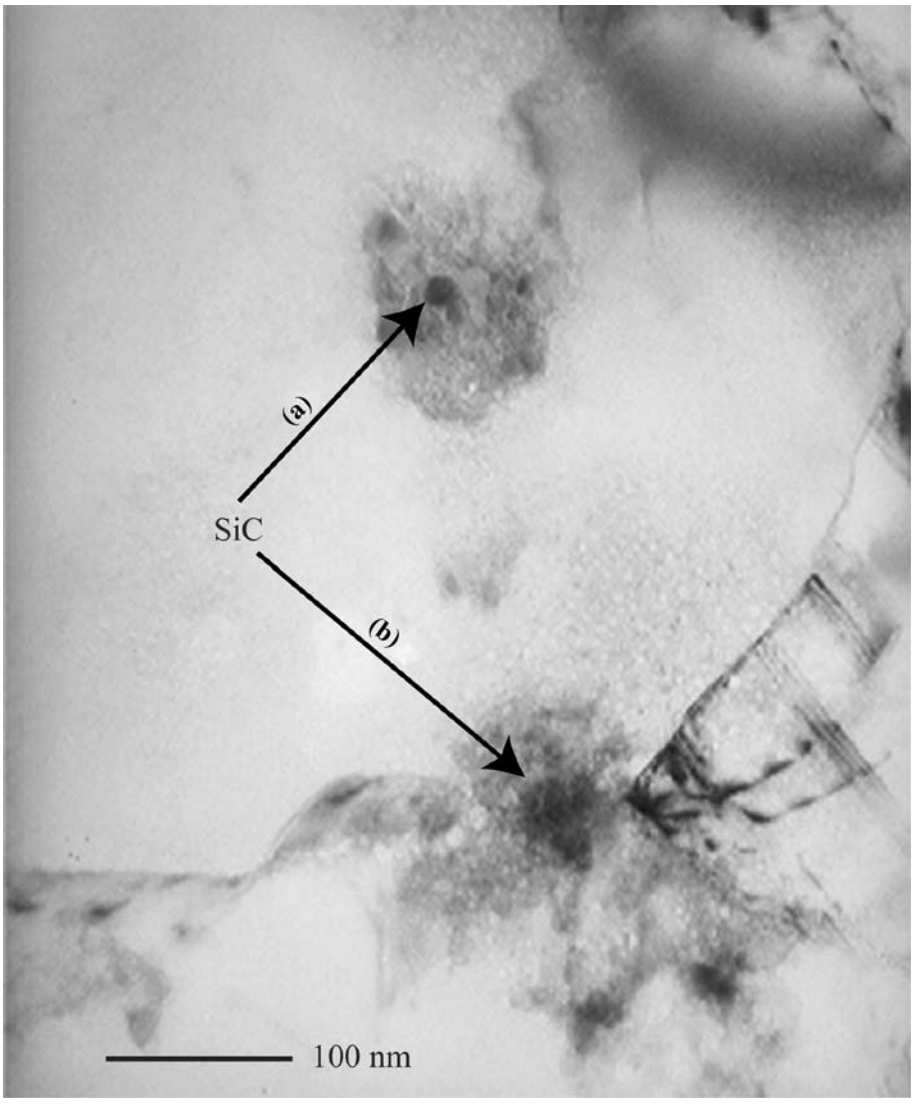

Fig. 9. TEM image of a cross section of a Ni/nano-SiC deposit prepared at d.c. = 70% presenting the partially intra-crystalline embedding of nano-SiC particles.

prepared under either direct or pulse current conditions with respect to pure nickel. The improved hardness of composite coatings may be associated to specific structural modifications of Ni crystallites due to local alkalization of the cathode/electrolyte interface produced by the adsorption of H^+ on the surface of SiC particles and therefore leading to a (211) mode of Ni crystal growth. Moreover, this type of inhibition of nickel electrocrystallization, which is more pronounced in the case of Ni/micron-SiC deposits, results in a reduction in grain size and an increased number of crystalline dislocations. The application of pulse electrodeposition significantly improved the hardness of the Ni/SiC composite coatings, especially at pulse-off times longer than pulse on-times, in which grain refinement and a higher incorporation SiC vol. % are achieved.

The effect of particle size on hardness has revealed that the highest values were obtained for Ni/nano-SiC composites. The enhanced hardness of Ni/nano-SiC deposits compared to Ni/micron-SiC composites may be attributed to the increasing values of number density of embedded SiC particles in the nickel matrix with decreasing particle size. Moreover, the hardness modifications produced by the codeposition of different sizes of SiC particles may be associated to different embedding mechanisms of the particles in the metal matrix, *i.e.* an inter-crystalline type of micron-SiC particles and partially intra-crystalline of nano-sized SiC particles. Additionally, the hardness increase noted in both kinds of Ni/SiC coating may also be linked to a dispersion strengthening mechanism.

Acknowledgement

Part of this work was funded by the European Commission (project InMan, contract BRPR-CT98–0788).

References

1. J. Fransaer, J.P. Celis and J.R. Roos, *Met. Finish.* **91** (1993) 97.
2. A. Hovestad and L.J.J. Janssen, *J. Appl. Electrochem.* **25** (1995) 519.
3. M. Musiani, *Electrochim. Acta* **45** (2000) 3397.
4. L. Orlovskaja, N. Periene, M. Kurtinaitiene and S. Surviliene, *Surf. Coat. Technol.* **111** (1999) 234.
5. P. Gyftou, E.A. Pavlatou, N. Spyrellis and K.S. Hatzilyberis, *Trans. Inst. Met. Finish.* **78** (2000) 223.
6. I. Garcia, J. Fransaer and J.-P. Celis, *Surf. Coat. Technol.* **148** (2001) 171.
7. A.F. Zimmerman, G. Palumbo, K.T. Aust and U. Erb, *Mater. Sci. Eng. A* **328** (2002) 137.
8. L. Benea, P.L. Bonora, A. Borello and S. Martelli, *Wear* **249** (2002) 995.
9. I. Garcia, A. Conde, G. Langelaan, J. Fransaer and J.P. Celis, *Corros. Sci.* **45** (2003) 1173.
10. S.H. Yeh and C.C. Wan, *J. Appl. Electrochem.* **24** (1994) 993.
11. G. Maurin and A. Lavanant, *J. Appl. Electrochem.* **25** (1995) 1113.
12. P. Gyftou, M. Stroumbouli, E.A. Pavlatou and N. Spyrellis, *Trans. Inst. Met. Finish* **80** (2002) 88.
13. A.F. Zimmermann, D.G. Clark, K.T. Aust and U. Erb, *Mater. Lett.* **52** (2002) 85.
14. S.K. Kim and H.J. Yoo, *Surf. Coat. Technol.* **108–109** (1998) 564.
15. S.-C. Wang and W.-C.J. Wei, *Mater. Chem. Phys.* **78** (2003) 574.
16. M.-D. Ger, *Mater. Chem. Phys.* **87** (2004) 67.
17. K.H. Hou, M.D. Ger, L.M. Wang and S.T. Ke, *Wear* **253** (2002) 994.
18. N.K. Shrestha, M. Masuko and T. Saji, *Wear* **254** (2003) 555.
19. P. Nowak, R.P. Socha, M. Kaisheva, J. Fransaer, J.-P. Celis and Z. Stoinov, *J. Appl. Electrochem.* **30** (2000) 429.
20. R.P. Socha, P. Nowak, K. Laajalehto and J. Väyrynen, *Coll. Surf. A* **235** (2004) 45.
21. M. Kaisheva and J. Fransaer, *J. Electrochem. Soc.* **151** (2004) C89.
22. F. Hu and K.C. Chan, *Appl. Surf. Sci.* **233** (2004) 163.
23. C. Kollia, N. Spyrellis, J. Amblard, M. Froment, M. Froment and G. Maurin, *J. Appl. Electrochem.* **20** (1990) 1025.
24. A.M. El-Sherik, U. Erb and J. Page, *Surf. Coat. Technol.* **88** (1996) 70.
25. E. Tóth-Kádár, I. Bakonyi, L. Pogány and Á Cziráki, *Surf. Coat. Technol.* **88** (1996) 57.
26. N.S. Qu, D. Zhu, K.C. Chan and W.N. Lei, *Surf. Coat. Technol.* **168** (2003) 123.
27. H.E. Boyer (ed.), *Hardness Testing* (ASM International, Metals Park, OH, 1987).
28. R. Mishra, B. Basu and R. Balasubramaniam, *Mater. Sci. Eng. A* **373** (2004) 370.
29. J. Amblard, M. Froment, G. Maurin and N. Spyrellis, *J. Microsc. Spectrosc. Electron.* **6** (1981) 311.
30. J. Amblard, Th. Costavaras, A. Hugot-Le Goff and N. Spyrellis, *Oberfläche-Surf.* **1** (1977) 18.
31. F. Denise and H. Leidheiser, *J. Electrochem. Soc.* **100** (1953) 490.
32. D.J. Evans, *Trans. Far. Soc.* **54** (1958) 1086.
33. A. Knödler, *Metalloberfläche* **20** (1966) 52.
34. C.S. Lin and K.C. Huang, *J. Appl. Electrochem.* **34** (2004) 1013.
35. J. Amblard, M. Froment and N. Spyrellis, *Surf. Technol.* **5** (1977) 205.
36. S. Psarrou, C. Kollia and N. Spyrellis, *Galvanotecnica e Nuove Finiture* **4** (1999) 224.
37. P. Gyftou, E.A. Pavlatou and N. Spyrellis, *Galvanotecnica e Nuove Finiture* **11** (2001) 23.